

Single molecule tracking of heterogeneous diffusion

Jianshu Cao

Department of Chemistry, Massachusetts Institute of Technology, Cambridge, Massachusetts 02139

(Received 27 November 2000; published 16 March 2001)

The mean square displacement of heterogeneous diffusion obeys the Einstein relation, thereby showing no sign of heterogeneities in the ensemble measurement of the diffusion constant. The signature of spatial heterogeneities appears in the time evolution of the non-Gaussian distribution and in the cross correlation between the square displacements at different times, both available from single molecule diffusional trajectories. As a quantitative measure, the non-Gaussian indicator $g(t)$ decays asymptotically to zero according to $1/t$ for finite time correlation, but saturates at a plateau value for power-law correlation. In addition, the joint moment correlation function $f(t, \tau)$ provides a direct probe of the memory effect of the fluctuating rate constant. A two-state diffusion model and a stochastic Gaussian model are constructed to evaluate these quantities and are shown to yield the same result within the second cumulant expansion.

DOI: 10.1103/PhysRevE.63.041101

PACS number(s): 82.20.Fd, 05.40.-a, 82.20.Db

I. INTRODUCTION

Single molecule detection and imaging has provided rich and detailed information about many fundamental physical processes [1–6]. Such information is often hidden in ensemble measurements but can be obtained from careful statistical analysis of single molecule data [7–13]. Several articles [14,15] have extensively reviewed the current progress of single molecule methods in various systems ranging from low-temperature amorphous solids to room-temperature enzymatic reactions. The focus of this paper is the single molecule detection of translational diffusion. Schmidt and co-workers have recorded translational diffusion trajectories of individual fluorescence-labeled lipid molecules in a fluid lipid membrane. They found anomalous diffusion consisting of a slow component and a fast component and interpreted their findings as a result of island structures of the membrane surrounded by barriers for lipid diffusion [16]. The diffusion trajectories of single dye molecules have also been recorded in polyacrylamide gels by Dickson and co-workers [17] and in solution by Xu and Yeung among others [18–20].

Anomalous translational diffusion is an intriguing topic in physics, chemistry, and biology. It has long been recognized that spatial heterogeneities are inherent in the dynamics of glass-forming systems including polymers, supercooled liquids, supercritical liquids, and colloidal fluids [21–25]. Zwanzig studied percolation in a dynamic disordered system using a two-zone diffusion model, where spherical domains of higher diffusivity than the background appear and disappear with a relaxation time τ [26–28]. Liu and Oppenheim applied the two-zone diffusion model to explain enhanced diffusion near the kinetic glass transition [29]. It was further suggested that the existence of long-lived spatial heterogeneities is responsible for the nonexponential α relaxation [30]. In a different context, Berne and Pecora used a set of coupled diffusion equations to describe light scattering from electrolyte solutions [31]. Dieterich and co-workers developed stochastic models and percolation concepts to study ion diffusion in complex systems [32]. In biophysics, the traditional fluid mosaic model describes the cell membrane as a two-dimensional oriented solution in viscous phospholipic pro-

teins. Recent revision of the mosaic model introduces considerable nanometer heterogeneities in the membrane structure [33,34]. Some proteins are transiently confined to small island domains bounded by obstacle clusters, and some undergo rapid and directed transport propelled by cytoskeletal motors. Single molecule tracking provides a powerful way to directly monitor the anomalous diffusion behavior.

We do not intend to cover all aspects of anomalous diffusion but will address features related to single molecule measurements. The classical theory of Brownian motion predicts a Gaussian distribution with a linear time dependence for the mean square displacement [35]. Conventional bulk experiments, analyzed with Brownian theory, often lead to ensemble-averaged diffusion constants. In contrast, single molecule experiments allow for the tracking of single particles, thus yielding the complete probability distribution of the displacement and the correlation function of Brownian motion at two different times. In heterogeneous environments, a Brownian particle travels through distinct diffusion areas of various sizes and geometrical arrangements. In our model, both static and dynamic heterogeneities of the medium translate into a distribution in diffusivity and a temporal correlation for the traced particle. Though an approximation of realistic systems, our simplified models capture some basic aspects of heterogeneous diffusion. A possible extension of the current analysis is to introduce regions of ballistic motion in the homogeneous or inhomogeneous background so that anomalous diffusion can be detected on the level of the mean square displacement.

The rest of the paper is organized as follows: Two single molecule quantities are introduced in Sec. II. These quantities are calculated for the stochastic Gaussian model in Sec. III, for the two-state diffusion model in Sec. IV, for the non-Poisson two-state diffusion model in Sec. V. Finally, concluding remarks are given in Sec. VI.

II. SINGLE MOLECULE MEASUREMENTS

In single molecule experiments, one can in principle follow the motion of individual Brownian particles and map out the probability distribution and correlation as a function of

time. A useful measure to quantify this distribution is the time-dependent spatial moment $I_n(t) = \langle |r(t) - r(0)|^n \rangle$. For simplicity, we consider diffusion in one-dimensional space; generalization to higher-dimensional space is straightforward. Since higher-order moments usually suffer from more statistical noise, we will study the first two nonvanishing moments $I_2(t)$ and $I_4(t)$. For a Gaussian distribution, higher-order moments are determined by the second moment, e.g., $I_4(s) = 3I_2^2(s)$; therefore, the deviation from the Gaussian distribution can be measured by $J(t) = I_4(t) - 3I_2^2(t)$. To scale $J(t)$, a non-Gaussian indicator is defined as

$$\sigma(t) = J(t) / 3I_2^2(t), \quad (1)$$

which was first introduced by Rahman in liquid argon simulations and has since been applied to various statistical treatments [36].

Within the models presented in this paper, the mean square displacement follows the Einstein relation for Brownian motion, $I_2(t) = 2\langle D \rangle t$, with the effective diffusion constant expressed as an inhomogeneous average. In general, the Brownian particle is randomly selected from the sample, and the initial diffusion is confined to one domain; therefore, the short-time distribution is simply an inhomogeneous average of Brownian motions over all domains. Consequently, the short-time limit of $I_4(t)$ can be expressed as $\lim_{t \rightarrow 0} I_4(t) = 3\langle (2Dt)^2 \rangle$, where $\langle D^2 \rangle$ denotes an inhomogeneous average. The initial value of $\sigma(t)$ is given explicitly as $\sigma(0) = \langle \delta D^2 \rangle / \langle D \rangle^2$, with $\langle \delta D^2 \rangle = \langle D^2 \rangle - \langle D \rangle^2$ the variance of the diffusion constant. Thus, the non-Gaussian indicator can be normalized as

$$g(t) = \frac{\sigma(t)}{\sigma(0)} = \frac{\langle D \rangle^2}{\langle \delta D^2 \rangle} \frac{J(t)}{3I_2^2(t)}, \quad (2)$$

which will be shown to be independent of the diffusion constant.

In single molecule experiments, one can track the diffusion process of a single particle and make multiple measurements along the Brownian trajectory. For example, the square displacements at two different times define the joint moment function

$$I(t_1, \tau, t_2) = \langle |r(t_1) - r(0)|^2 |r(\tau + t_1 + t_2) - r(\tau + t_1)|^2 \rangle, \quad (3)$$

where τ is the time separation of the two different measurements. Without the memory effect of the rate constant, the joint moment function is the product of two independent random displacements, i.e., $I(t_1, \tau, t_2) = I_2(t_1)I_2(t_2)$, with $I_2(t) = \langle |r(t) - r(0)|^2 \rangle$. Therefore, the memory effect of the rate constant can be quantified by the normalized correlation function of the square displacement

$$f(t, \tau) = \frac{I(t, \tau, t) - [I_2(t)]^2}{I(t, 0, t) - [I_2(t)]^2}, \quad (4)$$

which will be shown to be proportional to the memory function of the diffusion constant in the limit of $t \rightarrow 0$.

III. STOCHASTIC FLUCTUATION MODEL

Diffusion in homogeneous environments follows $\partial P(t, r) / \partial t = \nabla [D \nabla P(t, r)]$, where $P(t, r)$ is the probability density. The Fourier transformation of the diffusion equation gives $\partial P(t, k) / \partial t = -Dk^2 P(t, k)$, which is solved formally as $P(t, k) = \exp(-k^2 t D) P(0, k)$. The inhomogeneous environments experienced by a Brownian particle introduce time dependence in the diffusion constant. This time dependence can be treated as a stochastic process so that the spatial Fourier transform of the probability distribution is given as

$$P(t, k) = \left\langle \exp \left(-k^2 \int_0^t D(t') dt' \right) \right\rangle_s P(0, k). \quad (5)$$

The large brackets $\langle \dots \rangle_s$ in the above equation represent a stochastic average, which is characterized via a cumulant expansion

$$\begin{aligned} & \left\langle \exp \left(-k^2 \int_0^t D(t') dt' \right) \right\rangle_s \\ &= \exp \left[-k^2 \int_0^t dt_1 \chi_1(t_1) + k^4 \int_0^t \int_0^{t_1} \chi_2(t_1, t_2) dt_1 dt_2 \right. \\ & \quad \left. - k^6 \int_0^t \int_0^{t_1} \int_0^{t_2} \chi_3(t_1, t_2, t_3) dt_1 dt_2 dt_3 + \dots \right], \quad (6) \end{aligned}$$

where

$$\begin{aligned} \chi_1(t_1) &= \langle D(t_1) \rangle_s, \\ \chi_2(t_1, t_2) &= \langle [D(t_1) - \chi_1(t_1)][D(t_2) - \chi_1(t_2)] \rangle_s, \\ \chi_3(t_1, t_2, t_3) &= \langle [D(t_1) - \chi_1(t_1)][D(t_2) - \chi_1(t_2)] \\ & \quad - \chi_1(t_2)][D(t_3) - \chi_1(t_3)] \rangle_s, \end{aligned}$$

etc. In principle, all the cumulants must be included in Eq. (6) to accurately describe the stochastic fluctuations of the diffusion constant. In practice, the two single molecule quantities suggested in Sec. II, $g(t)$ and $f(t, \tau)$, are both fourth-order moments and can be evaluated with a cumulant expansion accurate to k^4 . Therefore, we truncate Eq. (6) to second order, giving

$$P(t, k) = \exp[-k^2 D_0 t + k^4 M(t)] P(0, k), \quad (7)$$

which represents a stochastic Gaussian model for heterogeneous diffusion. Here, the stationary condition of the stochastic process is assumed, $D_0 = \langle D \rangle_s$ is the first cumulant, $M(t) = \int_0^t (t-t') \chi(t') dt'$ is the second cumulant, and $\chi(t) = \langle [D(t) - D_0][D(0) - D_0] \rangle_s$ is the correlation function of the diffusion constant. Obviously, our model shares the same spirit as Kubo's stochastic line-shape theory [37]. It should be noted, however, Eq. (7) cannot be used for the evaluation of the distribution function, as the Gaussian model is valid only to the fourth order of k .

To proceed, we derive expressions for $g(t)$ and $f(t)$ within the stochastic Gaussian model. In general, moments

can be calculated from $P(t,k)$ as $I_n(t) = (-1)^n P^{(n)}(t,k=0)$; thus, from Eq. (7), we have $I_2(t) = 2D_0t$, $I_4(t) = 3(2D_0t)^2 + 24M(t)$, and $J(t) = 24M(t)$. The normalized non-Gaussian indicator in Eq. (2) is given explicitly as

$$g(t) = \frac{2M(t)}{t^2\chi(0)}. \quad (8)$$

In the long-time limit, the indicator decays as

$$\lim_{t \rightarrow \infty} g(t) = \frac{2}{t\chi(0)} \int_0^\infty \chi(t') dt' = \frac{\tau_c}{t}, \quad (9)$$

where τ_c is the characteristic time scale of the fluctuations. Within the stochastic model, the joint moment correlation function in Eq. (3) can be derived from

$$I(t_1, \tau, t_2) = \frac{\partial^2}{\partial k_1^2} \frac{\partial^2}{\partial k_2^2} \left\langle \exp \left[-k_1^2 \int_0^{t_1} D(t') dt' \right] \times \exp \left[-k_2^2 \int_{t_1+\tau}^{t_1+\tau+t_2} D(t'') dt'' \right] \right\rangle, \quad (10)$$

where the term in the angular brackets is the joint moment generating function. The Gaussian averaging of the generating function leads to $I(t_1, \tau, t_2) = 4D_0^2 t_1 t_2 + 4[M(t_1 + \tau + t_2) - M(t_1 + \tau) - M(t_2 + \tau) + M(\tau)]$, which, when substituted in Eq. (10), gives

$$f(t, \tau) = \frac{M(2t + \tau) - 2M(t + \tau) + M(\tau)}{M(2t) - 2M(t)}. \quad (11)$$

In the limit of small t , the normalized correlation function reduces to

$$\lim_{t \rightarrow 0} f(t, \tau) = \frac{\chi(\tau)}{\chi(0)}, \quad (12)$$

which provides a direct measure of the correlation function of the diffusion constant.

IV. TWO-STATE MODEL: POISSON KINETICS

For simplicity, we consider a model consisting of two regions with diffusion constants D_1 and D_2 , which are correlated through two state kinetics (see Fig. 1). The correlation is introduced in a similar fashion as in two-channel modulated reactions [4,12] or in random walk with dichotomous fluctuations [38]. In different contexts, related two-state diffusion models have been used to study dynamic percolation and light scattering in electrolyte solutions [28,29,31]. We first study a Poisson rate process, where the rate from D_1 to D_2 is γ_1 , and the rate from D_2 to D_1 is γ_2 . The two-state heterogeneous diffusion is described by

$$\dot{P}_1(t,k) = -(\gamma_1 + k^2 D_1) P_1(t,k) + \gamma_2 P_2(t,k), \quad (13)$$

$$\dot{P}_2(t,k) = -(\gamma_2 + k^2 D_2) P_2(t,k) + \gamma_1 P_1(t,k), \quad (14)$$

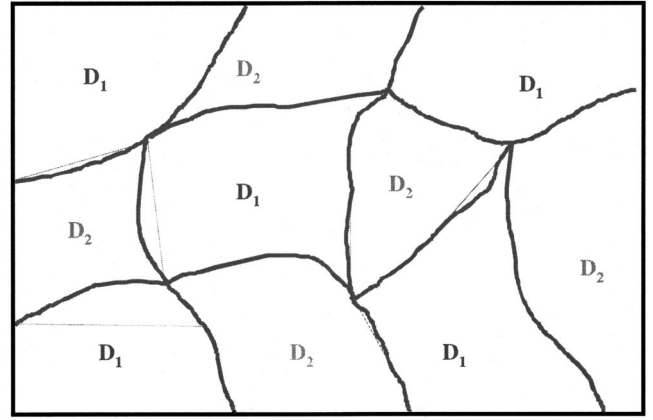


FIG. 1. A sketch of the two-state diffusive model for heterogeneous diffusion.

which after the Laplace transformation can be solved as

$$\begin{pmatrix} P_1(s,k) \\ P_2(s,k) \end{pmatrix} = \frac{1}{\text{Det}(s,k)} \begin{pmatrix} s + k^2 D_2 + \gamma_2 & \gamma_1 \\ \gamma_2 & s + k^2 D_1 + \gamma_1 \end{pmatrix} \times \begin{pmatrix} P_1(0,k) \\ P_2(0,k) \end{pmatrix}, \quad (15)$$

where the determinant is $\text{Det}(s,k) = (s + k^2 D_1 + \gamma_1)(s + k^2 D_2 + \gamma_2) - \gamma_1 \gamma_2$. The total probability distribution for the Brownian particle is $P(s,k) = P_1(s,k) + P_2(s,k)$ with the equilibrium distributions $P_1(0) = \gamma_2 / (\gamma_1 + \gamma_2)$ and $P_2(0) = \gamma_1 / (\gamma_1 + \gamma_2)$. For the special case of $\gamma_1 = \gamma_2 = \gamma$, the Fourier transform of the probability distribution is given by

$$P(t,k) = \exp[-(k^2 D_0 + \gamma)t] \times \left[\cosh(\Delta t) + \frac{\gamma}{\Delta} \sinh(\Delta t) \right] P(0,k), \quad (16)$$

where $D_0 = (D_1 + D_2)/2$ and $\delta = (D_1 - D_2)/2$ are the average and difference of the diffusion constants, and $\Delta^2 = k^4 \delta^2 + \gamma^2$. It is easy to confirm that the above expression reduces to the usual diffusion equation $P(t,k) = e^{-k^2 D_0 t} P(0,k)$ in the limit of $\delta \rightarrow 0$ or $\gamma \rightarrow \infty$. In Fig. 2, the probability distribution computed from Eq. (16) is plotted for the following set of parameters: $D_1 = 5$, $D_2 = 1$, $\gamma = 0.1$, and $t = 1$, along with a Gaussian distribution with the same average diffusion constant $D_0 = 3$. In comparison with the Gaussian curve, the probability distribution for the two-state diffusion model exhibits a higher center peak, a narrower width, and slower decay in the wings.

Next, we explicitly calculate $g(t)$ and $f(t, \tau)$ for the case of two-state Poisson kinetics. Directly from the probability distribution function in Eq. (16), we obtain

$$g(t) = \frac{\gamma t - e^{-\gamma t} \sinh(\gamma t)}{(\gamma t)^2}, \quad (17)$$

where the time variable is scaled by a single parameter γ . The normalized non-Gaussian indicator computed from Eq. (17) is plotted for $\gamma = 5$ and $\gamma = 1$ in Fig. 3, where the pre-

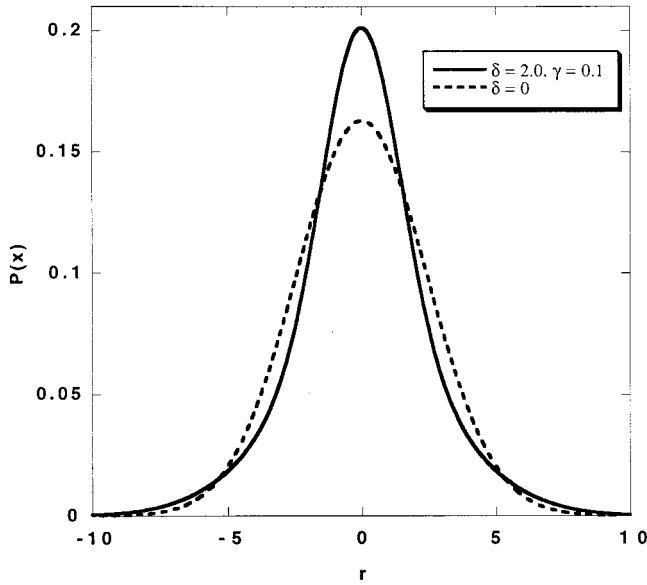


FIG. 2. A plot of the probability distribution (solid curve) computed from Eq. (16) for Poisson two-state diffusion with $D_1=5$, $D_2=1$, $\gamma=0.1$, and $t=1$. For comparison, a Gaussian distribution with the same mean square displacement is shown as the dashed curve.

dicted long-time asymptotic behavior of τ_c/t is clearly observed. The joint moment function in Eq. (3) is expressed as the product of three matrices

$$I(t_1, \tau, t_2) = \sum G_2(t_1)G_0(\tau)G_2(t_2)\rho_0, \quad (18)$$

where $G_2(t) = -\partial^2 G(t, k=0)$ is the second moment matrix and $G(\tau) = G(\tau, k=0)$ is the zero moment matrix. The ex-

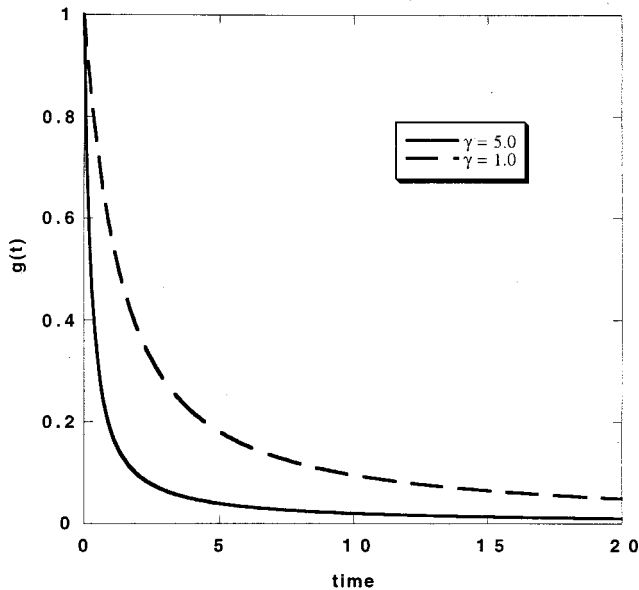


FIG. 3. A plot of the normalized non-Gaussian indicator $g(t)$ calculated from Eq. (17) for Poisson kinetics with $\gamma=5$ (solid curve) and $\gamma=1$ (dashed curve).

plicit expression for the propagator $G(k, s)$ in Eq. (15) allows us to evaluate $G_2(t)$ and $G_0(t)$, thus yielding $I(t_1, \tau, t_2) = 4D_0^2 t_1 t_2 + (D_1 - D_2)^2 E(t_1)E(t_2)e^{-2\tau\gamma}$, with $E(t) = e^{-\gamma t} \sinh(\gamma t)/\gamma$. Then, the normalized correlation function reads

$$f(t, \tau) = e^{-2\tau\gamma} \quad (19)$$

which is independent of time and the diffusion constant. As shown in Eq. (11), $f(t, \tau)$ is generally a function of time and reduces to $\chi(\tau)$ only in the limit of $t \rightarrow 0$, so Eq. (19) is a special case due to the exponential decay kinetics.

It is not coincident that the asymptotic limits of $g(t)$ and $f(t, \tau)$ in the two-state model are the same as predicted by the stochastic Gaussian model. In fact, with $\chi(t) = \exp(-2\gamma t)$, Eqs. (8) and (11) from the stochastic Gaussian model give exactly the same $g(t)$ and $f(t, \tau)$ as the two-state model. Furthermore, with identities $\chi(0) = \langle \delta D^2 \rangle = (D_1 - D_2)^2/4$ and $\langle D \rangle = (D_1 + D_2)/2$, all second and fourth moment functions are the same for the two models. It should be noted that the two models are not identical as their equivalence is not proven beyond the second-order cumulant expansion.

V. TWO-STATE MODEL: POWER-LAW KINETICS

To generalize the above formalism to non-Poisson kinetics, we need to specify $\psi_i(t)$, the waiting time probability in state i , or equivalently, $\phi_i(t) = -\dot{\psi}_i(t)$, the waiting time probability density in state i . First consider the case without diffusion. Assuming the initial distribution in state 1, the probability of finding the particle in the same state is

$$P_1(s) = \psi_1(s) + \psi_1(s)\phi_2(s)\phi_1(s) + \dots \\ = [1 - \phi_1(s)\phi_2(s)]^{-1}\psi_1(s), \quad (20)$$

where the first term represents the probability of staying in state 1 without any transition, the second term represents the probability of beginning in state 1 with a single sojourn in state 2, etc. Note that the Laplace transforms of $\phi(t)$ and $\psi(t)$ are related by $s\psi(s) - 1 = -\phi(s)$. The probability of finding the particle in state 2 is $P_2(s) = [1 - \phi_1(s)\phi_2(s)]^{-1}\phi_1(s)\psi_2(s)$, which satisfies the normalization condition $P_1(s) + P_2(s) = 1/s$. Similar results can be obtained for a particle starting from state 2. To incorporate spatial diffusion, $\psi(s)$ and $\phi(s)$ are generalized to $\Psi_i(s, k) = \psi_i(s + k^2 D_i)$ and $\Phi_i(s, k) = \phi_i(s + k^2 D_i)$, which are related by $(s + k^2 D_i)\Psi_i(s, k) - 1 = -\Phi_i(s, k)$. With the substitution of ψ and ϕ with Ψ and Φ , Eq. (20) can be modified to describe two-state spatial diffusion, yielding

$$\begin{pmatrix} P_1(s, k) \\ P_2(s, k) \end{pmatrix} = \frac{1}{1 - \Phi_1\Phi_2} \begin{pmatrix} \Psi_1 & \Phi_2\Psi_1 \\ \Phi_1\Psi_2 & \Psi_2 \end{pmatrix} \begin{pmatrix} P_1(0, k) \\ P_2(0, k) \end{pmatrix}, \quad (21)$$

which reduces to Eq. (15) for Poisson kinetics. Without any prior knowledge of the diffusion inhomogeneity, we take

$\phi_1(t) = \phi_2(t) = \phi(t)$ and the equilibrium distribution as $P_1(0) = P_2(0) = 1/2$. Then, the average distribution function is

$$P(s, k) = \frac{1}{2(1 - \Phi_1 \Phi_2)} \left[\frac{(1 - \Phi_1)(1 + \Phi_2)}{s + k^2 D_1} + \frac{(1 - \Phi_2)(1 + \Phi_1)}{s + k^2 D_2} \right], \quad (22)$$

where the initial condition is taken as $P(0, k) = 1$. Equation (22) describes the non-Gaussian distribution for a heterogeneous diffusion process.

With $P(s, k)$ in Eq. (22) as the generating function, we can evaluate all the moment functions. For example, the second moment is given by

$$I_2(s) = -\frac{\partial^2 P(s, k=0)}{\partial k^2} = \frac{D_1 + D_2}{s^2}, \quad (23)$$

which in real-time translates to $I_2(t) = (D_1 + D_2)t$. In general, the mean square displacement, as usually measured in bulk experiments, will not reveal the heterogeneity of the diffusion constant. The fourth-order moment is given by

$$I_4(s) = \frac{\partial^4 P(s, k=0)}{\partial k^4} = \frac{12}{s^3} \left[D_1^2 + D_2^2 + (D_1 - D_2)^2 \frac{s \phi'(s)}{1 - \phi^2(s)} \right], \quad (24)$$

which cannot be transformed to real time for an arbitrary waiting time distribution function. From Eqs. (23) and (24), we have

$$J(s) = \frac{6}{s^3} (D_1 - D_2)^2 \left[1 + \frac{2s \phi'(s)}{1 - \phi^2(s)} \right], \quad (25)$$

which depends quadratically on the difference of the diffusion constants. In the short-time limit of $t \rightarrow 0$, the second term in Eq. (25) can be ignored and we have

$$\lim_{t \rightarrow 0} J(t) = 3(D_1 - D_2)^2 t^2, \quad (26)$$

which predicts a quadratic time dependence. In combination with $I_2(t)$ in Eq. (23), the short-time limit of $I_4(t)$ can be expressed as $\lim_{t \rightarrow 0} I_4(t) = 6(D_1^2 + D_2^2)t^2 = 3\langle (2Dt)^2 \rangle$, where $\langle D^2 \rangle$ indicates an inhomogeneous average. Similar to Eq. (2), the initial value, $\sigma(0) = (D_1 - D_2)^2 / (D_1 + D_2)^2$, defines the normalized non-Gaussian indicator as

$$g(t) = \frac{\sigma(t)}{\sigma(0)} = \left(\frac{D_1 + D_2}{D_1 - D_2} \right)^2 \frac{J(t)}{3I^2(t)}, \quad (27)$$

which is independent of diffusion constants. The long-time asymptotic behavior of $g(t)$ or equivalently $J(t)$ has to be examined for two separated cases.

In the first case, the waiting time distribution $\phi(t)$ has a characteristic time scale τ_c such that $\phi(s)$ can be analyti-

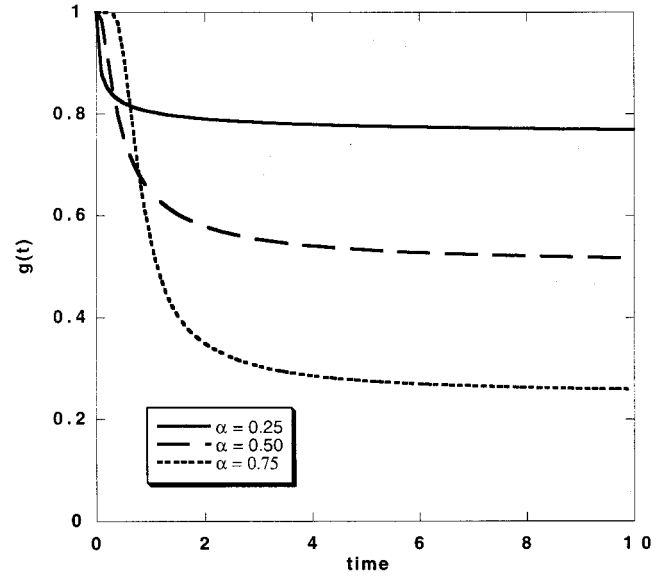


FIG. 4. A plot of the normalized non-Gaussian indicator $g(t)$ calculated from Eq. (31) for power-law kinetics with $\alpha = 0.25$, $\alpha = 0.5$, and $\alpha = 0.075$, respectively.

cally expanded as $\phi(s) = 1 + s \phi' + s^2 \phi''/2 + \dots$. To second order in the s expansion of $\phi(s)$, we obtain

$$J(s) \approx 3(D_1 - D_2)^2 \frac{\phi'(0)^2 - \phi''(0)}{s^2 \phi'(0)}, \quad (28)$$

which predicts a linear time dependence in $J(t)$ or, equivalently, $\lim_{t \rightarrow \infty} g(t) \propto 1/t$. With the definition $-\phi'(0) = \int \phi(t)t dt = \langle t \rangle$ and $\phi''(0) = \int \phi(t)t^2 dt = \langle t^2 \rangle$, the characteristic time scale τ_c can be explicitly expressed as $\tau_c = (\langle t^2 \rangle - \langle t \rangle^2) / \langle t \rangle$. This definition of τ_c is equivalent to Eq. (9) derived for the stochastic Gaussian model. Then, the linear deviation from the Gaussian behavior becomes

$$\lim_{t \rightarrow \infty} J(t) \approx 3(D_1 - D_2)^2 \tau_c t, \quad (29)$$

where $(D_1 - D_2)\tau_c$ characterizes the length scale of spatial heterogeneity. Comparing Eqs. (26) and (27), the transition from the short-time quadratic behavior to the long-time linear behavior in $J(t)$ takes place at $t \approx \tau_c$, which is another measure of the characteristic relaxation time.

In the second case, the waiting time distribution has diverging moments due to the lack of a characteristic time scale. In proteins and glassy systems, there exist a wide range of relaxation time scales, which can often be characterized by power-law decay [39]. A generic form of power-law relaxation is given in the Laplace form as

$$\phi(s) = \exp[-(s/\gamma)^\alpha], \quad (30)$$

which is not analytical at $s=0$ for $0 < \alpha < 1$. In real time, $\phi(t)$ is normalized to unity and decays at long times according to $1/t^{(1+\alpha)}$. Substituting $\phi(s)$ into Eq. (25) leads to

$$J(s) = \frac{6(D_1 - D_2)^2}{s^3} \left\{ 1 - \frac{2\alpha(s/\gamma)^\alpha \exp[-(s/\gamma)^\alpha]}{1 - \exp[-2(s/\gamma)^\alpha]} \right\} \quad (31)$$

which in the small- s limit reduces to $\lim_{s \rightarrow 0} J(s) = 6(D_1 - D_2)^2(1 - \alpha)/s^3$. Therefore, the asymptotic limit of the non-Gaussian indicator $g(t)$ does not decay to zero but reaches a plateau value of

$$\lim_{t \rightarrow \infty} g(t) = 1 - \alpha, \quad (32)$$

which is determined by the exponent of the power-law decay. In Fig. 4 the normalized non-Gaussian indicator computed from Eq. (31) is plotted as a function of time with $\gamma = 1$ for $\alpha = 0.25$, $\alpha = 0.5$, and $\alpha = 0.75$. After the initial decay, $g(t)$ approaches asymptotically the plateau value predicted by Eq. (32).

VI. CONCLUSIONS

Diffusion in heterogeneous environments obeys the Einstein relation for the mean square displacement but exhibits non-Gaussian distributions and memory effects, which can be measured through single molecular methods. Our model studies have led to the following conclusions.

(1) Two possible single molecule quantities are proposed: the normalized non-Gaussian indicator, $g(t)$, which quantifies the deviation from the Gaussian distribution of Brownian particles, and the normalized correlation function of square displacements, $f(t, \tau)$, which directly probes the memory effect of the fluctuating diffusion constant.

(2) In the same spirit as Kubo's stochastic line-shape theory, the stochastic Gaussian model captures essential features of heterogeneous diffusion. In particular, the long-time limit of $g(t)$ is shown to decay in the asymptotic form of τ_c/t , with τ_c being the characteristic time scale, and the short-time limit of $f(t, \tau)$ reproduces the memory function of the diffusion constant.

(3) The two-state diffusion model allows us to calculate the non-Gaussian distribution explicitly, thus confirming the asymptotic behavior of $g(t) = 1/\gamma t$ and the exponential decay of $f(t, \tau) = e^{-2\gamma t}$, where γ is the rate constant. It is interesting to note that the two-state diffusion model and the stochastic model are equivalent up to second order in the cumulant expansion.

(4) The two-state diffusion model can be generalized to non-Poisson kinetics, which is specified by the waiting time distribution function $\phi(t)$. For the power-law waiting time distribution with a long-time tail of $1/t^{(1+\alpha)}$, the non-Gaussian indicator $g(t)$ does not decay to zero but saturates at an asymptotic value of $(1 - \alpha)$.

In summary, the deviation from the usual Brownian behavior [40], as revealed by single molecule measurements, provides useful information about the variance and the scale of spatial inhomogeneities as well as the functional form of the long-range correlation function.

ACKNOWLEDGMENTS

The research is supported by the MIT start-up fund and NSF. The author thanks Younjoon Jung and Jianlan Wu for their help during the course of this work.

-
- [1] W. E. Moerner and M. Orrit, *Science* **283**, 1670 (1999).
 - [2] L. Edman, U. Mets, and R. Rigler, *Proc. Natl. Acad. Sci. U.S.A.* **93**, 6710 (1996).
 - [3] Y. Jia, A. Sytnik, L. Li, S. Vladimirov, B. S. Cooperman, and R. M. Hochstrasser, *Proc. Natl. Acad. Sci. U.S.A.* **94**, 7932 (1997).
 - [4] H. P. Lu, L. Xun, and X. S. Xie, *Science* **282**, 1877 (1998).
 - [5] T. Ha, A. Y. Ting, J. Liang, A. A. Deniz, D. S. Chemla, P. G. Schultz, and S. Weiss, *Chem. Phys.* **247**, 107 (1999).
 - [6] C. G. Baumann, V. A. Bloomfield, S. B. Smith, C. Bustanmante, M. D. Wang, and S. M. Block, *Biophys. J.* **78**, 1965 (2000).
 - [7] P. Reilly and J. L. Skinner, *Phys. Rev. Lett.* **71**, 4257 (1993).
 - [8] F. L. H. Brown and R. J. Silbey, *J. Chem. Phys.* **108**, 7434 (1998).
 - [9] J. Wang and P. Wolynes, *Phys. Rev. Lett.* **74**, 4317 (1995).
 - [10] E. Geva and J. L. Skinner, *Chem. Phys. Lett.* **288**, 225 (1998).
 - [11] K. Weston, P. J. Carson, H. Metiu, and S. K. Buratto, *J. Chem. Phys.* **109**, 7474 (1998).
 - [12] J. Cao, *Chem. Phys. Lett.* **327**, 38 (2000).
 - [13] N. Agmon, *J. Phys. Chem. B* **104**, 7830 (2000).
 - [14] T. Bache, W. E. Moerner, M. Orrit, and U. P. Wild, *Single-Molecule Optical Detection, Imaging and Spectroscopy* (VCH, Weinheim, 1996).
 - [15] X. S. Xie and J. K. Trautman, *Annu. Rev. Phys. Chem.* **49**, 441 (1998).
 - [16] G. J. Schutz, H. Schindler, and T. Schmidt, *Biophys. J.* **73**, 1073 (1997).
 - [17] R. M. Dickson, D. J. Norris, Y. L. Tzeng, and W. E. Moerner, *Science* **274**, 966 (1996).
 - [18] X. Xu and E. S. Yeung, *Science* **275**, 1106 (1997).
 - [19] T. Ha, J. Glass, T. Enderle, D. S. Chemla, and S. Weiss, *Phys. Rev. Lett.* **80**, 2093 (1998).
 - [20] M. A. Osborne, S. Balasubramanian, W. S. Futey, and D. Klennerman, *J. Phys. Chem. B* **102**, 3160 (1998).
 - [21] M. T. Cicerone and M. D. Ediger, *J. Chem. Phys.* **104**, 7210 (1996).
 - [22] B. J. Cherayil and M. D. Fayer, *J. Chem. Phys.* **107**, 7642 (1997).
 - [23] S. C. Tucker, *Chem. Rev.* **99**, 391 (1999).
 - [24] S. A. Egorov and J. L. Skinner, *J. Chem. Phys.* **112**, 275 (2000).
 - [25] G. Hinze, D. D. Brace, S. D. Gottke, and M. D. Fayer, *Phys. Rev. Lett.* **84**, 2437 (2000).
 - [26] A. K. Harrison and R. Zwanzig, *Phys. Rev. A* **32**, 1072 (1985).
 - [27] R. Zwanzig, *Proc. Natl. Acad. Sci. U.S.A.* **85**, 2029 (1988).
 - [28] R. Zwanzig, *Chem. Phys. Lett.* **164**, 639 (1989).

- [29] C. Z. W. Liu and I. Oppenheim, *Phys. Rev. E* **53**, 799 (1996).
- [30] M. Tokuyama, Y. Enomoto, and I. Oppenheim, *Phys. Rev. E* **56**, 2302 (1997).
- [31] B. J. Berne and R. Pecora, *Dynamic Light Scattering* (Wiley-Interscience, New York, 1976).
- [32] D. Dieterich, O. Durr, P. Pendzig, A. Bunde, and A. Nitzan, *Physica A* **266**, 229 (1999).
- [33] K. Jacobson, E. D. Sheets, and R. Simon, *Science* **268**, 1441 (1995).
- [34] F. L. H. Brown, D. M. Leitner, J. A. McCammon, and K. R. Wilson, *Biophys.* **78**, 125 (2000).
- [35] R. I. Cukier and J. M. Deutch, *Phys. Rev.* **177**, 240 (1969).
- [36] A. Rahman, *Phys. Rev.* **136**, A405 (1964).
- [37] R. Kubo, N. Toda, and N. Hashitsume, *Statistical Physics II* (Springer-Verlag, Berlin, 1985).
- [38] P. Allegrini, P. Grigolini, and B. J. West, *Phys. Rev. E* **54**, 4760 (1996).
- [39] G. Zumofen and J. Klafter, *Phys. Rev. E* **47**, 851 (1993).
- [40] B. Cut, B. Liu, and S. A. Rice (unpublished).